



# Treball Final de Grau

**Synthesis and characterization of coordination compounds with a fluorescent ligand.**

**Síntesis i caracterització de compostos de coordinació amb un lligand fluorescent.**

Lluís Artús Suàrez

*January 2015*



Aquesta obra esta subjecta a la llicència de:  
Reconeixement–NoComercial–SenseObraDerivada



<http://creativecommons.org/licenses/by-nc-nd/3.0/es/>



*Si he pogut veure més lluny que els altres, només és perquè em trobo sobre les espatlles de gegants.*

Isaac Newton

Només agrair aquest treball al GMMF per donar-me'n l'oportunitat; a la Dra. E. Carolina Sañudo per ser la meva tutora la qual m'ha ajudat en tot i sempre ha estat a punt per guiar-me amb la seva aclaparadora quantitat de coneixements; a els meus companys de laboratori, sempre a punt per a tot, amb un somriure a la boca; i per últim, gràcies als meus companys d'universitat i a la meva parella, els quals m'han ajudat a seguir tant en els moments incerts com en els moments de més feina.



**REPORT**





# CONTENTS

<b>1. SUMMARY</b>	<b>3</b>
<b>2. RESUM</b>	<b>5</b>
<b>3. INTRODUCTION</b>	<b>7</b>
<b>4. OBJECTIVES</b>	<b>11</b>
<b>5. EXPERIMENTAL SECTION</b>	<b>13</b>
5.1. Materials and methods	13
5.2. Synthesis of the Ligands ACRI-1 and ACRI-2 and complexes 1-5	13
5.2.1. Preparation of ACRI-1 ( $[\text{C}_{29}\text{H}_{23}\text{N}_3\text{O}_2]\cdot\text{HCl}$ )	13
5.2.2. Preparation of ACRI-2 ( $[\text{C}_{27}\text{H}_{19}\text{N}_3\text{O}_2]\cdot\text{HCl}$ )	13
5.2.3. Preparation of $[\text{Co}_2(\text{ACRI-1})_2]$ (complex 1)	14
5.2.4. Preparation of $[\text{Co}_2(\text{ACRI-2})_2]$ (complex 2)	14
5.2.5. Preparation of $[\text{Cu}_2(\text{ACRI-1})_2]$ (complex 3)	14
5.2.6. Preparation of $[\text{Cu}_2(\text{ACRI-2})_2]$ (complex 4)	15
5.2.7. Preparation of $[\text{Co}(\text{NO}_3)_2(\text{H}_2\text{O})_2]$ (complex 5)	15
5.3. Characterization techniques	15
<b>6. SYNTHESIS</b>	<b>17</b>
<b>7. RESULTS &amp; DISCUSSION</b>	<b>19</b>
7.1. Study of crystal structure	19
7.1.1. Complex 3 crystal structure discussion	19
7.1.2. Complex 5 crystal structure discussion	24
7.2. Electronic spectra	26
7.2.1. ACRI-2 UV-Vis spectrum	26
7.2.2. $[\text{Co}_2(\text{ACRI-2})_2]$ UV-Vis spectrum	27
7.2.3. $[\text{Cu}_2(\text{ACRI-1})_2]$ UV-Vis spectrum	27
7.3. Fluorescent properties	28
7.3.1. Complex 2 $[\text{Co}_2(\text{ACRI-2})_2]$ emission spectrum	29
7.3.2. Complex 3 $[\text{Cu}_2(\text{ACRI-1})_2]$ emission spectrum	29
7.4. $^1\text{H}$ NMR study	30
7.4.1. ACRI-1 $^1\text{H}$ NMR spectrum	30
7.4.2. ACRI-2 $^1\text{H}$ NMR spectrum	31
7.4.3. Complex 1 $^1\text{H}$ NMR paramagnetic spectrum	31

---

7.4.4. Complex $2^1\text{H}$ NMR paramagnetic spectrum	32
<b>8. CONCLUSIONS</b>	35
<b>9. REFERENCES AND NOTES</b>	37
<b>10. ACRONYMS</b>	39

# 1. SUMMARY

The Group of Magnetism and Functional Molecules (GMMF) at the Universitat de Barcelona has been researching the field of multifunctional magnetic and fluorescent molecules since 2012.<sup>1,2</sup> The fluorescent ligands ACRI-1 ( $[\text{C}_{29}\text{H}_{23}\text{N}_3\text{O}_2]\cdot\text{HCl}$ ) and ACRI-2 ( $[\text{C}_{27}\text{H}_{19}\text{N}_3\text{O}_2]\cdot\text{HCl}$ ) were designed in the group.<sup>3</sup> They are based in an acridine core (substituted or not) with two imino-phenol substituents. These ligands have a strong fluorescence and two coordination pockets that can coordinate 2 metals. This ligand combined to paramagnetic metals leads to the desired magnetic and fluorescent molecule.

Copper and cobalt complexes with ACRI-1 and ACRI-2 have been synthesized in this project. They have been characterized by Electrospray ionisation mass spectroscopy (ESI-MS), para and diamagnetic proton nuclear magnetic resonance ( $^1\text{H}$  RMN), infrared spectroscopy (IR), Ultraviolet-visible absorption spectroscopy, emission fluorescence spectroscopy and single crystal X-ray diffraction.

The synthesis of the published complex 1 ( $[\text{Co}_2(\text{C}_{29}\text{H}_{21}\text{N}_3\text{O}_2)_2]^{3+}$ ) and the reported complex 2 ( $[\text{Co}_2(\text{C}_{27}\text{H}_{17}\text{N}_3\text{O}_2)_2]^{1,3,4}$ ) have been successfully reproduced. The new species complex 3 ( $[\text{Cu}_2(\text{C}_{29}\text{H}_{21}\text{N}_3\text{O}_2)_2]^{3+}$ ) has been obtained crystallized in a supra-molecular porous structure with hexagonal channels, and it is a new fluorescent magnetic porous material.

**Keywords:** multifunctional molecules, fluorescent, magnetic, porous materials, copper, cobalt.



## 2. RESUM

El grup de magnetisme i molècules funcionals (GMMF) de la Universitat de Barcelona ha estat investigant el camp de les molècules multifuncionals magnètiques i fluorescents des del 2012.<sup>1,2</sup> Els lligands fluorescents ACRI-1 ( $[\text{C}_{29}\text{H}_{23}\text{N}_3\text{O}_2]\cdot\text{HCl}$ ) i ACRI-2 ( $[\text{C}_{27}\text{H}_{19}\text{N}_3\text{O}_2]\cdot\text{HCl}$ ) van ser dissenyats al grup.<sup>3</sup> Estan basats en un nucli d'acridina (substituïda o no) amb dos grups imino-phenol a cada extrem. Aquests lligands tenen una forta fluorescència i dos llocs de coordinació que poden coordinar dos metalls. Aquest lligand combinat amb metalls paramagnètics genera la molècula magnètica i fluorescent que buscàvem.

Durant aquest treball s'han dut a terme les síntesis de complexos de coure i de cobalt amb lligands ACRI-1 i ACRI-2. S'han caracteritzat per tècniques d'espectroscopia de masses amb ionització per electrospray (ESI-MS), ressonància magnètica nuclear para i diamagnètica de protó ( $^1\text{H}$  RMN), espectroscopia d'infraroig (IR), espectroscopia d'absorció ultraviolat-visible, espectroscopia d'emissió fluorescent i per difracció de raig X d'un cristall únic.

S'ha aconseguit reproduir el complex ja publicat com el complex 1 ( $[\text{Co}_2(\text{C}_{29}\text{H}_{21}\text{N}_3\text{O}_2)_2]$ )<sup>3</sup> i el citat complex 2 ( $[\text{Co}_2(\text{C}_{27}\text{H}_{17}\text{N}_3\text{O}_2)_2]$ ).<sup>1,3,4</sup> També s'ha aconseguit cristal·litzar per primera vegada el complex 3 ( $[\text{Cu}_2(\text{C}_{29}\text{H}_{21}\text{N}_3\text{O}_2)_2]$ )<sup>3</sup> el qual ho fa en una estructura porosa supra-molecular amb canals hexagonals. És, per tant, un nou material fluorescent, magnètic i porós.

**Paraules clau:** molècules multifuncionals, fluorescent, magnètic, porós, canals, ACRI, Cu, Co.



### 3. INTRODUCTION

New materials have been investigated by humans since our origins, always looking for windows to new properties and applications. They started from using stones to copper, iron, and steel; discovering the magnetism of magnetite and the bioluminescence of the firefly and finished with piezoelectric and thermoelectric materials, liquid crystals, semiconductors, and materials that could lead to spintronics.<sup>5</sup>

Multifunctional materials are a very interesting research area since our world is always asking for cheaper, faster and more complex devices. These materials open new possibilities to do the same or even more with less.

One example of multifunctional materials are those with magnetic and fluorescent properties. Magnetism and fluorescence are independent and unrelated properties but with the proper molecule they can coexist: In the last few years researchers from the GMMF at UB and from Institut des Sciences Chimiques de Rennes at Université de Rennes have achieved these materials by combining the fluorescence of a conjugated ligand (Acridine yellow derivatives<sup>1,3,4</sup>, 4,5-bis(propylthio)tetrathiafulvalene-N,N'-phenylenebis-(salicylideneimine)<sup>6</sup> and curcuminoid derivatives<sup>2</sup>) shown in Figure 01, and two or more paramagnetic ions <sup>1,2,3,4,6</sup> ( $\text{Cu}^{2+}$ ,  $\text{Fe}^{2+}$ ,  $\text{Co}^{2+}$ ,  $\text{Ni}^{2+}$ ,  $\text{Dy}^{3+}$ ,  $\text{Yb}^{3+}$ ,  $\text{Er}^{3+}$ ). Some  $\text{Y}^{3+}$  complexes have been synthesized in order to perform quantum-chemical calculations and to corroborate the absorption properties.<sup>6</sup>

The potential applications of fluorescent and magnetic molecules could be i.e. track the magnetic behaviour of a system if they were part of it. Ligands with large conjugated systems could be used for electronic transport at the nanoscale level making them the perfect candidates for electronic circuits and the attachment of appropriate metallic centres will introduce additional features as well as making these complexes a good bet for future electronics. If Lanthanides are used, the applications could go further, including chelate lasers, efficient organic light-emitting diodes (OLEDs) and polymer light-emitting diodes (PLEDs).<sup>6</sup>

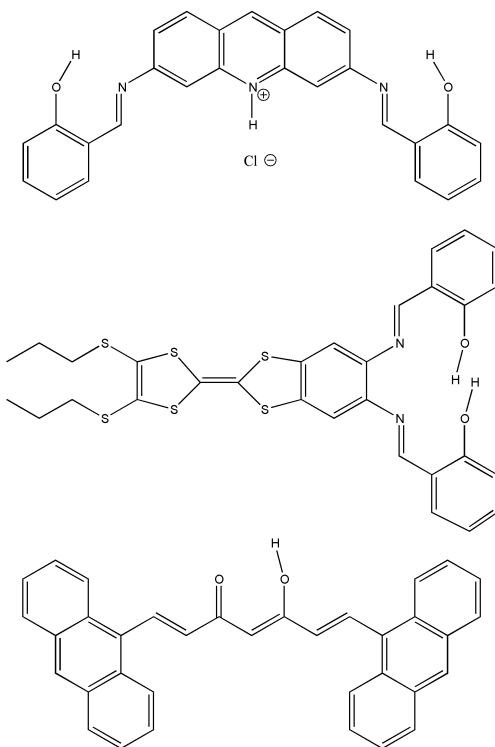


Figure 01. From top to bottom: ACRI-1, 4,5-bis(propylthio)tetrathiafulvalene-N,N'-phenylenebis(salicylideneimine), Curcume derivative (9 Accm).

Combining metals with fluorescent ligands in one molecule could have a constructive or destructive effect on the fluorescent properties: The chelation of a paramagnetic metal with a fluorescent ligand decreases the fluorescent intensity in contrast with diamagnetic metals like  $\text{Zn}^{2+}$  that enhance the fluorescent intensity. This is well known and reported in the literature<sup>2,3</sup> and the phenomenas are known as chelation enhancement of quenching (CHEQ) and chelation enhancement of fluorescence (CHEF).

The conjugated ligands can usually form excimers: excimers are aggregates, usually by  $\pi$ - $\pi$  stacking, of two or more complexes with one in an excited state; an illustration is shown in Figure 02. These aggregates can exhibit fluorescence when returning to their ground state. The fluorescent wavelength is higher than the normal fluorescence of the isolated conjugated system. They normally exist only on solid state or in concentrated solution and are short lived.



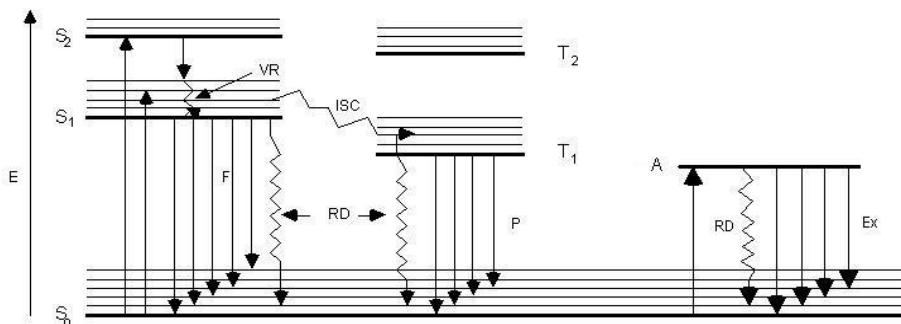


Figure 02. Description of fluorescence, phosphorescence and excimer emission origin. F, fluorescence; P, phosphorescence; S, singlet; T, triplet; RD, radiation less deactivation; VR, vibrational relaxation; ISC, intersystem crossing; A, aggregate of two complexes with one in an excited state; Ex, Excimer deactivation by photon emission; E, energy.<sup>7</sup> Image from Professor Monzir Abdel-Latif webpage. It has been modified.

Most of the metals used are Lanthanides. That is because lanthanides are not magnetic metals only, they are fluorescent too and this enhances the complex's properties.<sup>2,3,6</sup> There are even reports of heterobimetallic dinuclear and tetranuclear complexes that go further and combine the d metal's properties and the f metal's properties<sup>6</sup>.

Some other compounds with magnetic/fluorescent multifunctionality present another property: curcuminoids/Dy<sup>3+</sup> or curcuminoids/Yb<sup>3+</sup> are very interesting complexes because of its fluorescence single ion magnet (SIMs) behaviour.<sup>2</sup> They can be deposited on HOPG surfaces too. All this properties make them very interesting in the electronic world and could have a successful trajectory in this field if sufficiently improved.

There are more desired properties in this new world's devices like to be small and light. The only way to achieve this is to build with smaller and lighter components. Light components would be those with a low crystal density that are found in nanofibers, nanotubes, nanochannels, porous structures... All of them are relatively rare because Nature tends to fill all the empty spaces, but they can occur if it is possible to reduce the crystal energy. This can be achieved by hydrogen bonds,  $\pi$ - $\pi$  stacking, steric hindrance and the formation of macrocycles.



## 4.OBJECTIVES

This work follows a research line at GMMF: more specifically in the part of the synthesis of a family of fluorescent and magnetic complexes. Her work was motivated by the idea that combining a fluorescent ligand and a paramagnetic metal their characteristics would coexist together.

Since that work was not only centred in these complexes, some of them were not completely characterized. Because of this, this TFG study objective is to reproduce the cobalt and copper members of this family with the ACRI-1 and ACRI-2 ligands ( $[\text{C}_{29}\text{H}_{23}\text{N}_3\text{O}_2]\cdot\text{HCl}$  and  $[\text{C}_{27}\text{H}_{19}\text{N}_3\text{O}_2]\cdot\text{HCl}$  respectively), crystallize, determine its crystal structure (by single crystal diffraction), and characterize them by IR, NMR, UV-Vis and fluorescence. An additional objective is to try to extend this family.



## 5. EXPERIMENTAL SECTION

### 5.1. MATERIALS AND METHODS

All chemicals were purchased from commercial sources and used as received.

### 5.2. SYNTHESIS OF THE LIGANDS ACRI-1 AND ACRI-2 AND COMPLEXES 1-5

#### 5.2.1. Preparation of ACRI-1 ( $[\text{C}_{29}\text{H}_{23}\text{N}_3\text{O}_2]\cdot\text{HCl}$ )

Salicylaldehyde (854  $\mu\text{L}$ , 7.99 mmol) was slowly added to a  $\text{CH}_3\text{CH}_2\text{OH}$  solution (100 ml) of Acridine Yellow G ( $\text{C}_{15}\text{H}_{15}\text{N}_3\cdot\text{HCl}$ ) (1.215 g, 3.99 mmol). Then triethylamine (2.81 ml, 19.95 mmol) was added and the solution heated up to 79  $^\circ\text{C}$ . Reflux was maintained with stirring for 7 h. After standing 2 days, a precipitate was filtered, washed with ethanol, and dried with diethyl ether. The yield of the reaction was 93.6% (1.801 g) of a yellow-orange precipitate. IR (KBr pellet): 1605.56, 1567.68, 1495.41, 1462.05, 1384.36, 1352.95, 1277.67, 1186.79, 1132.20, 1030.15, 1004.64, 918.91, 847.76, 752.50, 635.80, 543.11, 452.41  $\text{cm}^{-1}$ .  $^1\text{H}$  NMR ( $\text{CDCl}_3$ , 400 MHz):  $\delta$  13.12 (s, 1H), 8.79 (s, 2H), 8.59 (s, 1H), 7.84 (s, 2H), 7.81 (s, 2H), 7.81 (s, 2H), 7.49-7.43 (m, 4H), 7.08 (d, 2H), 7.01 (t, 2H), 2.61 (s, 6H) LRMS (ESI):  $m/z$   $[\text{ACRI-1+H}]^+$  446.1864.

#### 5.2.2. Preparation of ACRI-2 ( $[\text{C}_{27}\text{H}_{19}\text{N}_3\text{O}_2]\cdot\text{HCl}$ )

Salicylaldehyde (826  $\mu\text{L}$ , 7.73 mmol) was slowly added to a  $\text{CH}_3\text{CH}_2\text{OH}$  solution (100 ml) of 3,6-Diaminoacridine hydrochloride ( $\text{C}_{13}\text{H}_{11}\text{N}_3\cdot\text{HCl}$ ) (1.0 g, 3.87 mmol). Then triethylamine (2.72 ml, 19.33 mmol) was added and the solution heated up to 79  $^\circ\text{C}$ . Reflux was maintained with stirring for 7 h. After standing 2 days, a precipitate was filtered, washed with ethanol, and dried with diethyl ether. The yield of the reaction was 54.7% (1.064 g) of a yellow-orange precipitate. IR (KBr pellet): 1602.76, 1567.66, 1497.63, 1486.27, 1458.12, 1399.24, 1360.36, 1319.34, 1288.93, 1222.89, 1169.68, 1153.68, 1132.72, 912.46, 904.01, 877.13, 846.29, 798.43, 775.13, 743.89, 732.58, 644.58, 468.69  $\text{cm}^{-1}$ .  $^1\text{H}$  NMR ( $\text{CDCl}_3$ , 400 MHz):  $\delta$  13.14 (s, 1H), 8.93 (s, 2H), 8.86 (s, 1H), 8.14 (d, 2H), 8.07 (s, 2H), 7.64 (d, 2H), 7.56-7.50 (m, 4H), 7.16 (d, 2H), 7.08 (t, 2H), LRMS (ESI):  $m/z$   $[\text{ACRI-2+H}]^+$  418.15.

### 5.2.3. Preparation of [Co<sub>2</sub>(ACRI-1)<sub>2</sub>] (complex 1)

An acetonitrile solution (20 ml) of ACRI-1 (0.25 g, 0.52 mmol) and Co(NO<sub>3</sub>)<sub>2</sub>·6H<sub>2</sub>O (0.16 g, 0.55 mmol) was prepared. Then triethylamine (0.24 ml, 1.68 mmol) was added and stirred 24 h. A precipitate was filtered, washed with acetonitrile and dried with diethyl ether. The yield of the reaction was 19.2% (106 mg) of brown precipitate. Crystals were obtained by slow evaporation of a chloroform solution of precipitate. 49 mg of complex 1 crystals were obtained (8.8%). IR (KBr pellet): 1604.37, 1574.00, 1528.33, 1456.88, 1434.04, 1381.24, 1354.67, 1319.32, 1243.56, 1184.98, 1162.57, 1148.12, 1132.07, 1102.58, 1027, 1003.60, 977.74, 916.78, 877.16, 850.63, 756.56 cm<sup>-1</sup>. <sup>1</sup>H NMR Paramagnetic (CDCl<sub>3</sub>, 400 MHz): δ 57.06 (s, 4H), 51.30 (s, 4H), 9.12 (s, 4H), 4.63 (s, 4H), 1.40 (s, 4H), -3.08 (s, 2H), -10.20 (s, 4H), -37.93 (s, 4H), -38.99 (s, 4H) LRMS (ESI): *m/z* [Co<sub>2</sub>(ACRI-1)<sub>2</sub>]<sup>+</sup>(triethylammonium) 1108.67 (due to a triethylamine spectrometer contamination).

### 5.2.4. Preparation of [Co<sub>2</sub>(ACRI-2)<sub>2</sub>] (complex 2)

An acetonitrile solution (20 ml) of ACRI-2 (0.313 g, 0.69 mmol) and Co(NO<sub>3</sub>)<sub>2</sub>·6H<sub>2</sub>O (0.2 g, 0.69 mmol) was prepared. Then triethylamine (0.29 ml, 2.06 mmol) was added and stirred 20 h. A precipitate was filtered, washed with acetonitrile and dried with diethyl ether. The yield of the reaction was 85.3% (279 mg) of a brown precipitate. Crystals were obtained by slow evaporation of a chloroform solution of precipitate. 7 mg of complex 2 crystals were obtained (2.1%). IR (KBr pellet): 1604.18, 1574.12, 1526.95, 1505.68, 1486.60, 1448.23, 1383.65, 1316.35, 1171.23, 1147.07, 1031.19, 975.87, 911.67 876.65, 863.96, 809.88, 798.54, 754.89, 644.81, 574.48, 517.89, 469.10 cm<sup>-1</sup>. <sup>1</sup>H NMR Paramagnetic (CDCl<sub>3</sub>, 400 MHz): δ 58.36 (s, 4H), 50.92 (s, 4H), 8.00 (s, 4H), 7.48 (s, 4H), 7.02 (s, 2H), -6.39 (s, 4H), -7.79 (s, 4H), -35.12 (s, 4H), -46.58 (s, 4H) LRMS (ESI): *m/z* [Co<sub>2</sub>(ACRI-2)<sub>2</sub>+H]<sup>+</sup> 949.14.

### 5.2.5. Preparation of [Cu<sub>2</sub>(ACRI-1)<sub>2</sub>] (complex 3)

An acetonitrile solution (20 ml) of ACRI-1 (0.154 g, 0.32 mmol) and CuCl<sub>2</sub>·2H<sub>2</sub>O (0.052 g, 0.031 mmol) was prepared. Then triethylamine (0.156 ml, 0.92 mmol) was added and stirred 26 hours. A precipitate was filtered, washed with acetonitrile and dried with diethyl ether. The yield of the reaction was 96.3% (149 mg) of a brown precipitate. Crystals were obtained by evaporation of a chloroform solution of precipitate. 8 mg of complex 3 brown hexagonal crystals were obtained (5.2%). IR (KBr pellet): 1605.19, 1582.83, 1529.46, 1495.81, 1455.95, 1434.89,

1383.40, 1353.19, 1320.35, 1249.79, 1187.89, 1151.87, 1133.15, 1029.43, 1003.81, 931.90, 868.22, 758.72, 636.97, 572.53, 539.77, 49.68, 446.18 cm<sup>-1</sup>. LRMS (ESI):  $m/z$  [Cu<sub>2</sub>(ACRI-1)<sub>2</sub>+H]<sup>+</sup> 1015.19.

### 5.2.6. Preparation of [Cu<sub>2</sub>(ACRI-2)<sub>2</sub>] (complex 4)

An acetonitrile solution (20 ml) of ACRI-2 (0.266g, 0.586mmol) and CuCl<sub>2</sub>·2H<sub>2</sub>O (0.100g, 0.587mmol) was prepared. Then triethylamine (0.245 ml, 1.740mmol) was added and stirred 26 hours. A precipitate was filtered, washed with acetonitrile and dried with diethyl ether. The yield of the reaction was 59.14% (166 mg) of brown precipitate. Crystals were obtained by evaporation of a chloroform solution of precipitate. 10 mg of complex 4 crystals were obtained (3.6%). IR (KBr pellet): 1605.27, 1588.83, 1531.06, 1505.61, 1486.69, 1468.22, 1449.46, 1383.13, 1319.82, 1172.74, 1147.97, 1029.42, 985.88, 916.40, 865.30, 810.44, 757.80, 661.48, 636.96, 575.35, 520.62 cm<sup>-1</sup>. LRMS (ESI):  $m/z$  [Cu<sub>2</sub>(ACRI-2)<sub>2</sub>+H]<sup>+</sup> 957.1291, [Cu<sub>2</sub>(ACRI-2)<sub>2</sub>]<sup>+</sup>Na<sup>+</sup> 979.11.

### 5.2.7. Preparation of [Co(NO<sub>3</sub>)<sub>2</sub>(H<sub>2</sub>O)<sub>2</sub>] (complex 5)

An acetonitrile solution (20 ml) of ACRI-2 (0.313 g, 0.69 mmol) and Co(NO<sub>3</sub>)<sub>2</sub>·6H<sub>2</sub>O (0.200 g, 0.69 mmol) was prepared. Then pyridine (0.169 ml, 2.07 mmol) was added and stirred 18 hours. A precipitate was filtered, washed with acetonitrile and dried with diethyl ether. Complex 2 was obtained. The mother liquor was separated and settled a week. After it 5 mg (33.1%) of brown complex 5 crystals were obtained.

## 5.3. CHARACTERIZATION TECHNIQUES

Infrared spectra have been collected on a KBr pellets on an AVATAR 330 FT-IR at Departament de Química Inorgànica, Universitat de Barcelona. X-Ray diffractions have been collected on a Bruker APEXII SMART diffractometer using Molybdenum K $\alpha$  microfocus ( $\lambda=0.71073$  Å) radiation source. The structures were resolved by direct methods (SHELXS97) and refined in F<sub>2</sub> (SHELX-97). The hydrogen atoms were included in the calculated in function of the bonding atoms. The NMR-<sup>1</sup>H measurements were carried by the NMR services of CCIT-UB. The UV-Vis spectra were acquired on a Cary 100 Scan de Varian at Departament de Química Inorgànica, Universitat de Barcelona. The fluorescence measurements were taken with a NanoLog™-Horiba JobinYvon iHR320 spectrometer.





## 6. SYNTHESIS

The ligands used in this work were designed at GMMF. ACRI-1 and ACRI-2 are based in acridine yellow and proflavine respectively (they are who provide the fluorescence to the ligands) through Schiff base formation with salicylaldehyde (see Figure 03). These ligands are ditopics with two separate coordination pockets that are far enough to avoid quenching of the fluorescence of the central fluorophore by coordination to a metal atom.

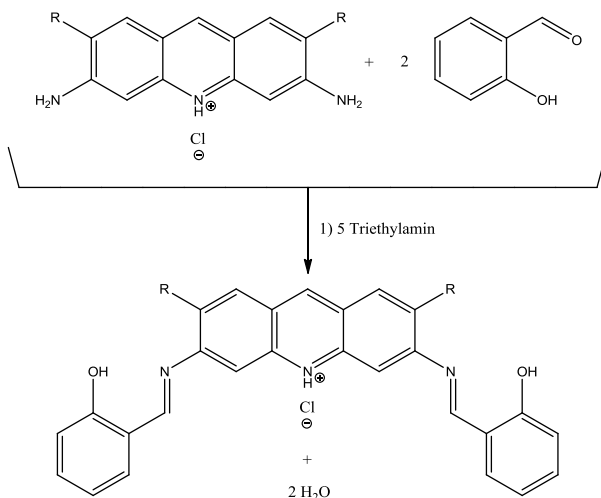


Figure 03. Imine formation by condensation in ethanol. R = CH<sub>3</sub> (ACRI-1) or H (ACRI-2).

To reproduce complexes 1, 2, 3 and 4, reactions of one of the two ligands (ACRI-1 and ACRI-2) with one of the two metals (Co(NO<sub>3</sub>)<sub>2</sub>·6H<sub>2</sub>O and CuCl<sub>2</sub>·2H<sub>2</sub>O) in MeCN were done. The result is an impurified precipitate of the desired complex. To purify it, crystallization by slow evaporation of a chloroform complex solution is needed.

In an attempt to obtain complexes with the ACRI-1 and ACRI-2 ligands and hexacoordinated metals, triethylamine was replaced for pyridine in the reaction of formation of complex 1-4 reaction. Complex 5 was obtained from the reaction of Co(NO<sub>3</sub>)<sub>2</sub>·6H<sub>2</sub>O with ACRI-1 and pyridine after discarding a precipitate and by slow evaporation of the mother liquor in the

case of the complex 2 reaction by settling the mother liquor a week. Two nitrate ions, two pyridine ligands and two residual waters coordinate the metal forming an octahedral complex. The discarded precipitate was identified by IR as complex 2.

## 7. RESULTS&DISCUSSION

### 7.1. STUDY OF CRYSTAL STRUCTURE

#### 7.1.1. Complex 3 crystal structure discussion

Table 01 contains the crystallographic data and structural parameters for complex3 ( $[\text{Cu}_2(\text{ACRI-1})_2]$ ). The complex 3 crystallizes in the triclinic space group and the crystal structure is shown in Figure 04. There is only  $\frac{1}{2}$  a molecule of complex 3 in the asymmetric unit contrary to their analogous complex 1 that consist on 2 half of 2 molecules of ( $[\text{Co}_2(\text{ACRI-1})_2]$ ) (see Figure 05).<sup>1</sup> The two copper atoms are tetracoordinated in a very distorted geometry, half-way between tetrahedral and square planar. The intramolecular Cu-Cu distance is 12.188 Å. The acridine core of the ligand ACRI-1 displays parallel-displaced intramolecular  $\pi$ - $\pi$  stacking. The shortest distance between acridines units is 3.181 Å. The distance between the two acridines nitrogen is 3.335 Å. Hydrogens atoms from two of solvent chloroforms groups participate in hydrogen bonding with the acridine nitrogen from complex 3. The supramolecular crystal structure is kept together by 3 types of intermolecular interactions: hydrogen bonds between the phenol oxygen and the acidic hydrogen of the chloroform solvent molecules and by two types of intermolecular  $\pi$ - $\pi$  stacking between the phenol rings at 3.507 Å and 3.524 Å (see Figure 06). These intermolecular interactions provide a very porous crystal structure with hexagonal channels of 9.5x12 Å filled with chloroform solvent molecules (see Figure 07). Even with the chloroform molecules filling the channel, there is an empty space of 4.7x7.0 Å (see Figure 08). Because of this, complex 3 crystals have a hexagonal shape (Figure 09). If activated these channels could possibly adsorb gasses or cations. Chloroform molecules could also be replaced by some convenient molecule once the structure is formed to modify the channels properties. Since these channels are directed to a single direction, it is provable that the material could have some kind of anisotropy.

<b>Empirical formula</b>	C <sub>66</sub> H <sub>50</sub> Cl <sub>24</sub> Cu <sub>2</sub> N <sub>6</sub> O <sub>4</sub>
<b>Formula weight [g/mol]</b>	1969.098 (±0.009)
<b>T [K]</b>	296(2) (ambient temperature)
<b>Crystal system</b>	Triclinic
<b>Space group</b>	P1
<b>a, b, c [Å]</b>	11.3396(17), 13.7000(19), 15.079(3)
<b>α, β, γ [°]</b>	110.514(9), 107.670(9), 94.263(12)
<b>V [Å<sup>3</sup>]</b>	2047.2(5)
<b>Z</b>	2
<b>ρ<sub>calc</sub> [mg·mm<sup>-3</sup>]</b>	2.159
<b>F (000)</b>	1346
<b>Crystal size [μm]</b>	213x250x170
<b>Goodness-of-fit on F<sup>2</sup></b>	1.307
<b>Final R indexes [I &gt; 2σ(I)]</b>	0.0879
<b>Final R indexes [all data]</b>	0.1589
<b>Radiation type</b>	Mo Kα radiation source

Table 01. Crystal data and structure refinement for [Cu<sub>2</sub>(ACRI-1)<sub>2</sub>·8CHCl<sub>3</sub>.

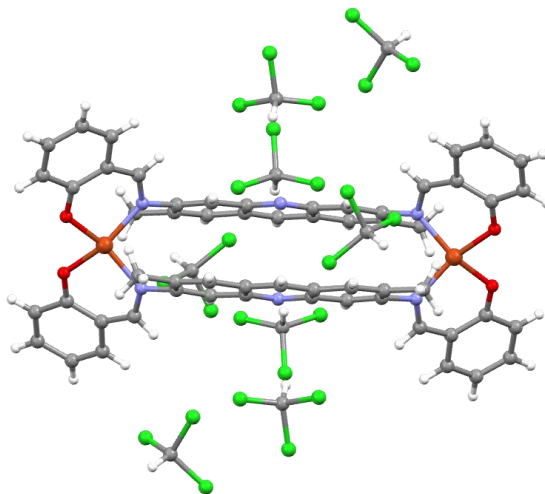


Figure 04. Crystal structure of the complex [Cu<sub>2</sub>(ACRI-1)<sub>2</sub>·8CHCl<sub>3</sub>. Carbon: grey, nitrogen: blue, oxygen: red, hydrogen: white, copper: orange, chlorine: green.

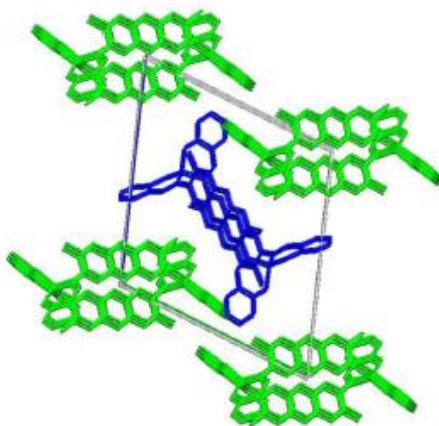


Figure05. Packing diagram in which the two crystallographically independent dinuclear units of complex 1 are shown in green and blue.

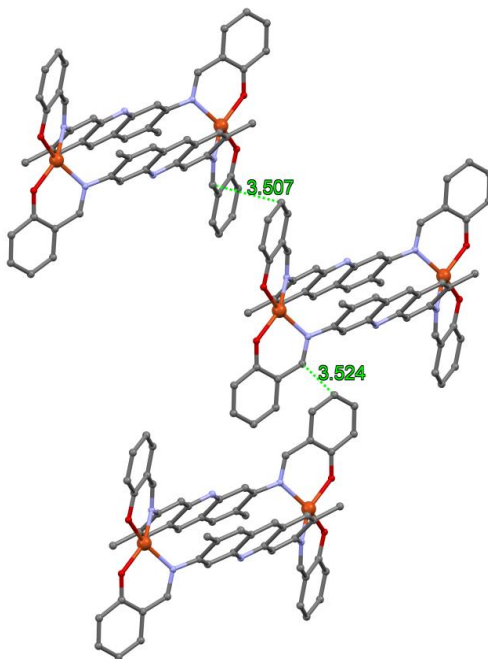


Figure 06. Intermolecular  $\pi$ - $\pi$  stacking. Atom-Atom distance (Å) shown in green.

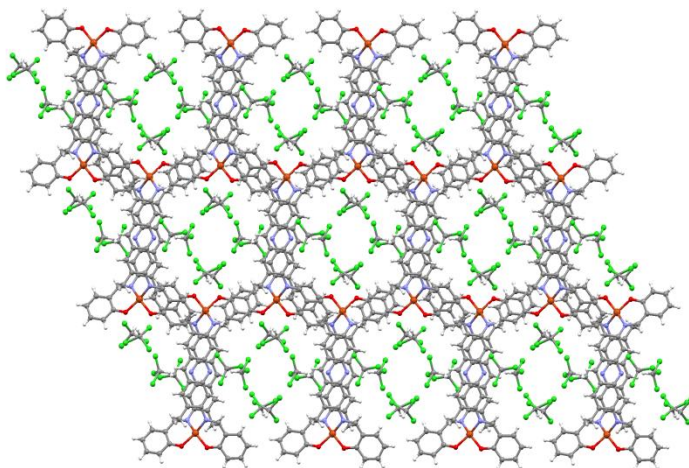


Figure 07. Complex 1's channels' crystal structure.

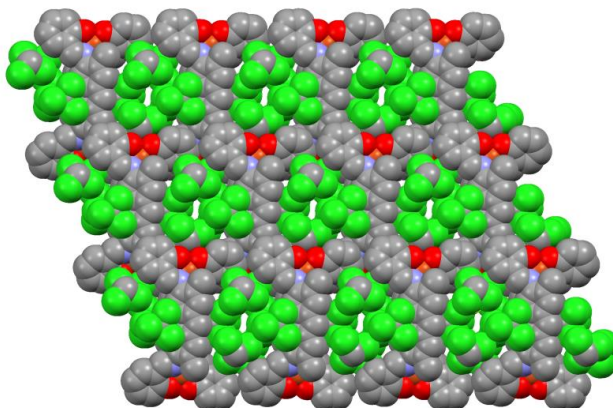


Figure 08. Channels spacefilling.



Figure 09. Complex 3 crystal photo.

The crystal structure of complex 1 ( $[\text{Co}_2(\text{ACRI-1})_2]$ ) was previously reported in a GMMF paper.<sup>1</sup> It will be discussed here again so a comparison with complex 3 can be done.

The complex 1 crystallizes in the triclinic space group P-1. As said before, this molecule exhibits two non-related by symmetry molecules species. The asymmetric unit contains two half molecules (Co1 and Co2) with a torsion angle  $\text{Co1-Co1}'\cdots\text{Co2-Co2}'$  of  $112^\circ$  (Co1' and Co2' are the symmetry related atoms to Co1 and Co2). The metal has a tetrahedral coordination with the ligands.  $\pi$ - $\pi$  stacking happens between the acridine cores with a minimum distance of  $3.190 \text{ \AA}$  (between acridine nitrogen)

The differences in the crystal packing of complex 1 and complex 3 is one of the most unexpected things found in this research: they have the same type and number of ligands, both complexes formed the  $\text{M}_2(\text{ligand})_2$  dimer with 3d metals in the oxidation state 2+, but nevertheless the crystal packing is completely different.

One feature that could be relevant in determining which packing happens is that ligand-metal bonds from complex 1 are almost all of them larger than ligand-metal bonds from complex 3 (see Table 002). Another one could be that copper shows a greater ease in forming square-planar disposition than cobalt (Table 02 shows copper angles approach much more to  $90^\circ$  and  $180^\circ$  than cobalt). This two could be the responsible of complex 3 phenol groups to line up more parallel with acridine ring plane: complex 1 deviation is  $66.57^\circ$  and the deviation of complex 3 is  $41.78^\circ$  (see Figure 10). In this manner phenol  $\pi$ - $\pi$  stacking becomes easier.

	Complex 1	Complex 3
<b>Distances (Å)</b>		
N1-M	2.004	1.986
N2-M	1.995	1.973
O1-M	1.898	1.910
O2-M	1.908	1.896
<b>Angle (°)</b>		
N1-M-N2	108.41	97.63
N2-M-O1	96.40	93.36
O1-M-O2	113.86	87.34
O2-M-N1	95.42	92.96
N1-M-O1	121.01	153.60
N2-M-O2	123.68	154.09

Table 02. Comparison chart between complex 1 and complex 3 measurements.

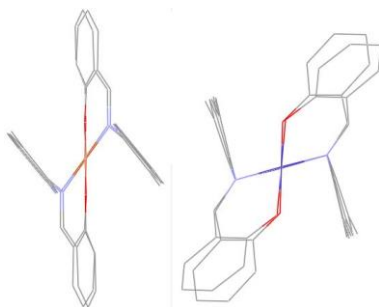


Figure 10. Complex 3 and Complex 1 crystal structure comparison. Complex 3 on the left, Complex 1 on the right.

### 7.1.2. Complex 5 crystal structure discussion

Table 03 contains the crystallographic data and structural parameters for complex 5  $[\text{Co}(\text{H}_2\text{O})_2(\text{NO}_3)_2(\text{py})_2]$ . The complex 5 crystallizes in the monoclinic space group and the crystal structure is shown in Figure 11. There is only  $\frac{1}{2}$  a molecule of complex 5 in the asymmetric unit. The ligands are hexacoordinated in a very clear octahedral geometry. The distribution of the different ligands is: the two waters face by face in a trans configuration, the two nitrates in a trans configuration too and bonded by the oxygen and the two pyridines in trans bonded by the nitrogen. Hydrogens atoms from the waters form intermolecular hydrogen bonds with the nitrates oxygens fixing the crystal structure. The unit cell consists on a cube where each vertex is formed with a cobalt atom. There is a cobalt atom in the centre of two opposite faces also



(see Figure 12). The vertex molecules are rotated 60° in the b/c plane and 90 in the a coordinate in relation to face molecules (see Figure 12 again).

<b>Empirical formula</b>	C <sub>10</sub> H <sub>14</sub> CoN <sub>4</sub> O <sub>8</sub>
<b>Formula weight [g/mol]</b>	377.1728 (±0.0001)
<b>T [K]</b>	296(2) (ambient temperature)
<b>Crystal system</b>	Monoclinic
<b>Space group</b>	P 21/c
<b>a, b, c [Å]</b>	8.8736(5), 11.7586(6), 7.5456(4)
<b>α, β, γ [°]</b>	90, 107.304(3), 90
<b>V [Å<sup>3</sup>]</b>	751.68(7)
<b>Z</b>	1
<b>ρ<sub>calc</sub> [mg·mm<sup>-3</sup>]</b>	1.808
<b>F (000)</b>	1346
<b>Crystal size [μm]</b>	130×130×80
<b>Goodness-of-fit on F<sup>2</sup></b>	0.975
<b>Final R indexes [I &gt; 2σ(I)]</b>	0.0336
<b>Final R indexes [all data]</b>	0.0406
<b>Radiation type</b>	Mo Kα radiation source

Table 03. Crystal data and structure refinement for [Co(H<sub>2</sub>O)<sub>2</sub>(NO<sub>3</sub>)<sub>2</sub>(py)<sub>2</sub>].

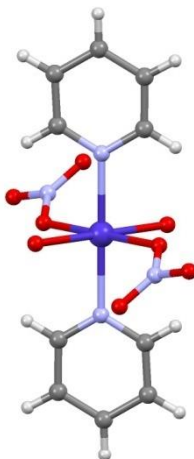


Figure 11. Crystal structure of the complex 5. Carbon: grey, nitrogen: blue, oxygen: red, hydrogen: white, cobalt: violet. Water's hydrogens are not represented because of single crystal X-ray diffraction is a technique that cannot localize them.

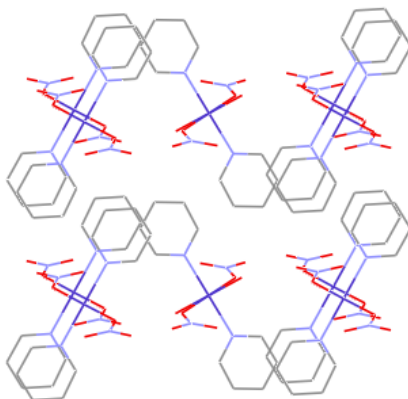


Figure 12. Complex 5 packing diagram. Carbon: grey, nitrogen: blue, oxygen: red, hydrogen: white, cobalt: violet.

## 7.2. ELECTRONIC SPECTRA

UV-Vis spectra were collected for the ligand ACRI-2, complex 2 and complex 3.

### 7.2.1. ACRI-2 UV-Vis spectrum

Figure 13 shows the electronic spectra of ACRI-2. From 200 to 420 nanometres absorbance of the aromatic groups can be observed as the combination of the phenol ring and the acridine unit. ACRI-2 had to be diluted to  $10^{-5}$  M to avoid saturation of the signal and to obtain good resolution since it has very intense yellow colour.

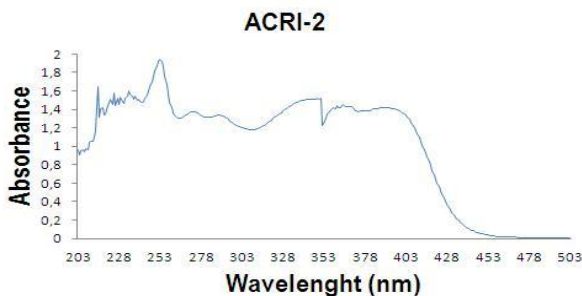


Figure 13. ACRI-2 spectra from a  $5 \cdot 10^{-5}$  M solution.

### 7.2.2. $[\text{Co}_2(\text{ACRI-2})_2]$ UV-Vis spectrum

Complex 2 is brown. Its electronic spectrum showed the same aromatic absorbance characteristic of the free ligand at a concentration of  $10^{-5}$  M, but slightly shifted due to the coordination, as shown in Figure 14. Cobalt tetrahedral complexes have forbidden d-d bands dominated by the highest energy transition  $^4\text{A}_2 \rightarrow ^4\text{T}_1(\text{P})$ .<sup>8</sup> They are visible from 550 to 680 if a more concentrated solution ( $10^{-3}$  M) is measured as shown in Figure 15, but the ligand absorption bands are saturated.

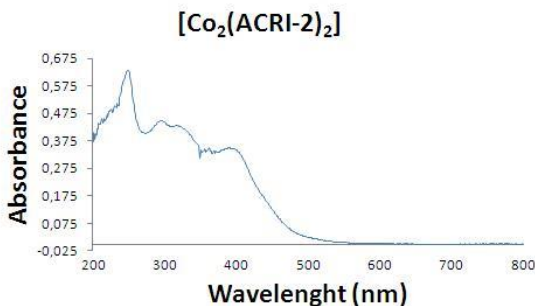


Figure 14.  $[\text{Co}_2(\text{ACRI-2})_2]$  spectrum from a  $8 \cdot 10^{-6}$  M solution.

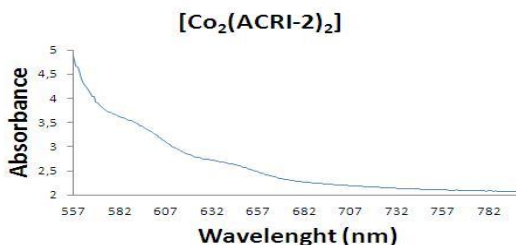


Figure 15.  $[\text{Co}_2(\text{ACRI-2})_2]$  spectrum from a  $3 \cdot 10^{-3}$  M solution. Metal bands detail.

### 7.2.3. $[\text{Cu}_2(\text{ACRI-1})_2]$ UV-Vis spectrum

Complex 3 exhibits a brown colour too. Free ligands bands are a little more distorted than in complex 2 as shown in Figure 16. The metal based d-d absorption bands that are forbidden are visible when concentrated solutions are irradiated, as shown in Figure 17. Because of the relatively low symmetry of the environment in which the  $\text{Cu}^{2+}$  ion is found, detailed interpretation of the spectra is somewhat complicated.<sup>8</sup> Usually  $\text{Cu}^{2+}$  complexes are blue or green but these

ones are exceptions caused by strong uv bands—charge-transfer bands—tailing off into the blue end of the visible spectrum, thus causing the substances to appear red or brown.<sup>8</sup>

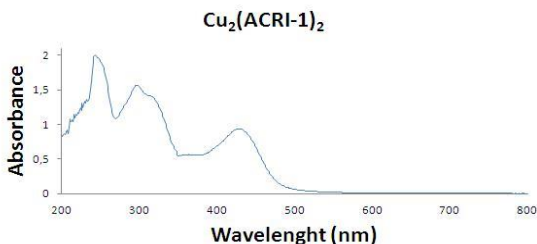


Figure 16.  $[\text{Cu}_2(\text{ACRI-1})_2]$  spectrum from a  $7 \cdot 10^{-6}$  M solution.

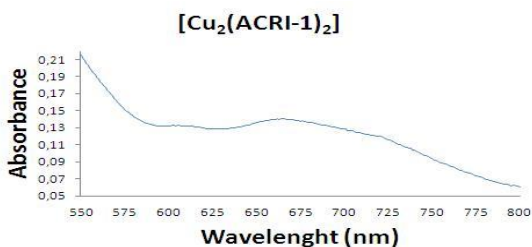


Figure 17.  $[\text{Cu}_2(\text{ACRI-1})_2]$  spectrum from a  $5 \cdot 10^{-5}$  M solution. Metal bands detail.

### 7.3. FLUORESCENT PROPERTIES

The complexation of ACRI-1 and ACRI-2 with copper and cobalt should lead to a quenching of the fluorescent properties of the free ligand, however it is expected from what GMMF previously reported on complex 1 that the fluorescence is still quite intense. Thus, emission spectra were collected for the prepared complexes.

The fluorescence of the complexes of this work is based on the excimer emission phenomena.<sup>9</sup> Acridine core is the complex responsible of the excimer. The 350 nm wavelength radiation was selected to excite the solutions. Since this wavelength corresponds to a free ligand band, it is assumed that the observed bands are based on the ligand. Samples were solubilized in chloroform. Emitted radiation was measured at 90 degrees in relation to excitation radiation.

### 7.3.1. Complex 2 [Co<sub>2</sub>(ACRI-2)<sub>2</sub>] emission spectrum

Emission spectra were collected at different concentrations for complex 2. At high concentrations the signal was saturated: if there is a high concentration, new deactivations paths are possible and excimer emissions appear at low energies. Complex 1, 2, 3 and 4 are intramolecular excimers that cannot be broken diluting. At a 10<sup>-4</sup> M concentration the emission signal for complex 2 was observed at 550 nm with two shoulders (one at 500 nm and the other at 600 nm) (as shown in Figure 18). The signal at 700 nm is the excitation radiation harmonic.

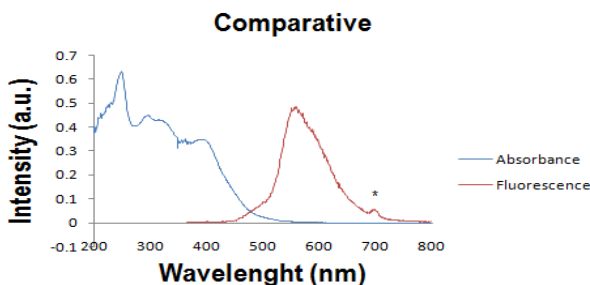


Figure 18. Complex 2 comparative graph of absorbance and fluorescence. Excitation radiation harmonic is marked with a \*.

### 7.3.2. Complex 3 [Cu<sub>2</sub>(ACRI-1)<sub>2</sub>] emission spectrum

Emission spectra were collected for complex 3 at different concentrations. At 10<sup>-4</sup> M concentration the excimer emission band saturated the detector and at 10<sup>-5</sup> M concentration it had very low intensity. A 3·10<sup>-5</sup> M solution had to be prepared to observe properly this emission band. A broad ligand-based emission band at 550 nm was observed when the sample was irradiated with a 350 nm light beam (see Figure 19).

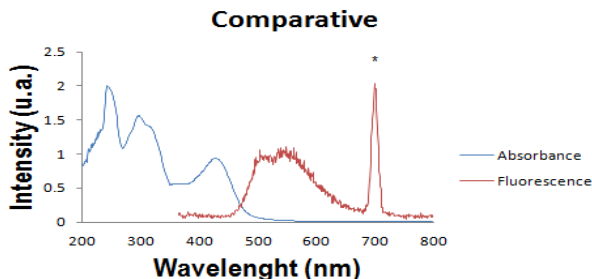


Figure 19. Comparative graph of absorbance and fluorescence for complex 3. Excitation radiation harmonic is marked with a \*.

## 7.4. $^1\text{H}$ NMR STUDY

### 7.4.1. ACRI-1 $^1\text{H}$ NMR spectrum

The  $^1\text{H}$  NMR spectrum of the ligand ACRI-1 was taken in  $\text{CDCl}_3$  to ensure that reaction went correctly and to prove its purity. ACRI-1 has 11 different types of hydrogens. Only 10 ligand hydrogens could be distinguished experimentally since the phenolic proton is in fast exchange with the dissolvent. The protio-impurity of the  $\text{CDCl}_3$  solvent is marked with an asterisk. Contamination solvent peaks from diethyl ether, water and acetonitrile were seen in the spectrum. (Figure 20).

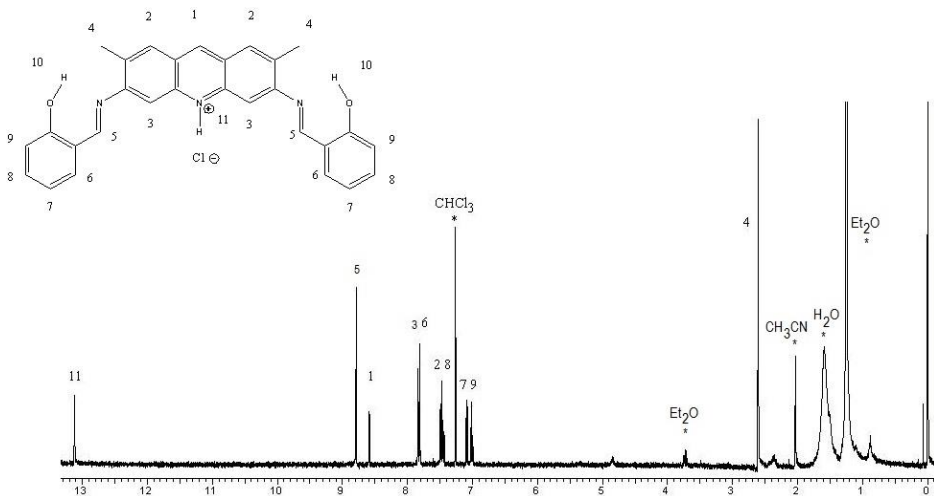


Figure 20. ACRI-1  $^1\text{H}$  NMR spectrum.

#### 7.4.2. ACRI-2 $^1\text{H}$ NMR spectrum

The ACRI-2  $^1\text{H}$  NMR in  $\text{CDCl}_3$  spectrum was measured to check purity, the spectrum is showed in Figure 21. It has 11 different types of hydrogens. ACRI-2 spectrum is basically as ACRI-1 one but with a little difference: the hydrogen number 4. Where before there was a methyl group, now there is only hydrogen. This move some signals, a signal that integrated 6 disappears, and a signal that integrate 2 appears.

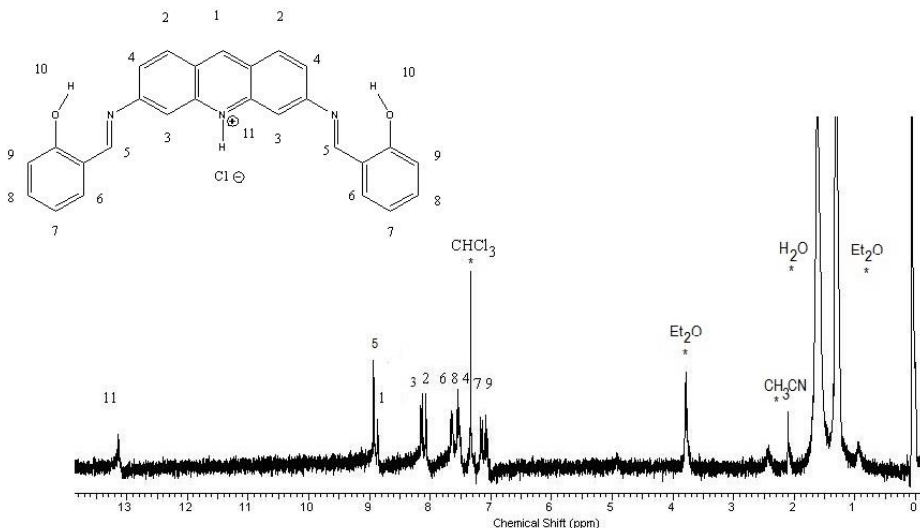


Figure 21. ACRI-2  $^1\text{H}$  NMR spectrum.

#### 7.4.3. Complex 1 $^1\text{H}$ NMR paramagnetic spectrum

Paramagnetic  $^1\text{H}$  NMR is not very common but it can be used with great success to study  $\text{Co(II)}$  complexes due to the strong dipolar coupling characteristic of  $\text{Co(II)}$ . Only elements with low gyromagnetic constant offer well resolved spectrum with large paramagnetic shifts and sharp peaks.  $^1\text{H}$  NMR paramagnetic spectra cannot be used to identify hydrogen coupling since it has very broad signals because the metal intervene in the magnetic environment that the hydrogens receive and because they not only couple through bonds but also through space. Since Co has a lower gyromagnetic constant than Cu, only Complex 1 and complex 2 paramagnetic  $^1\text{H}$  NMR spectra have been collected.

For complex 1 there are nine types of hydrogen atoms, thus nine peaks must be seen. Ortho hydrogens are very close in space to the Co and shifted to high fields. Meta hydrogens

are shifted to low fields. The hydrogen atoms of the ACRI-1 ligand central acridine unit should not be so affected by the metal since they are relatively far from it. Figure 22 shows the paramagnetic NMR of complex 1. The protio-impurity of the  $\text{CDCl}_3$  solvent is marked with an asterisk.

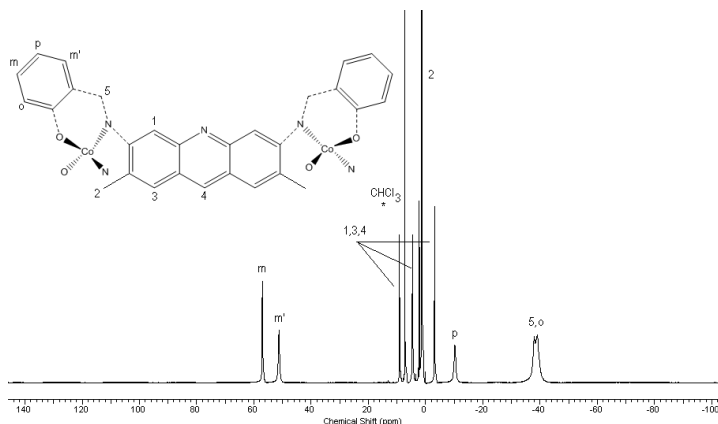


Figure 22. Complex 1  $^1\text{H}$  NMR paramagnetic spectrum. Protio impurity of the  $\text{CDCl}_3$  solvent is marked with asterisk.

#### 7.4.4. Complex 2 $^1\text{H}$ NMR paramagnetic spectrum

Complex 2 spectrum is basically like that of complex 1 but without the methyl groups of the central acridine yellow unit which are now protons (see Figure 22). Free ACRI-2 impurities which are diamagnetic are clearly seen from 7 to 13 ppm: the false doublets from 7 to 9.5 ppm and the sharp signal at 13 (from ACRI-2 hydrogen 11).



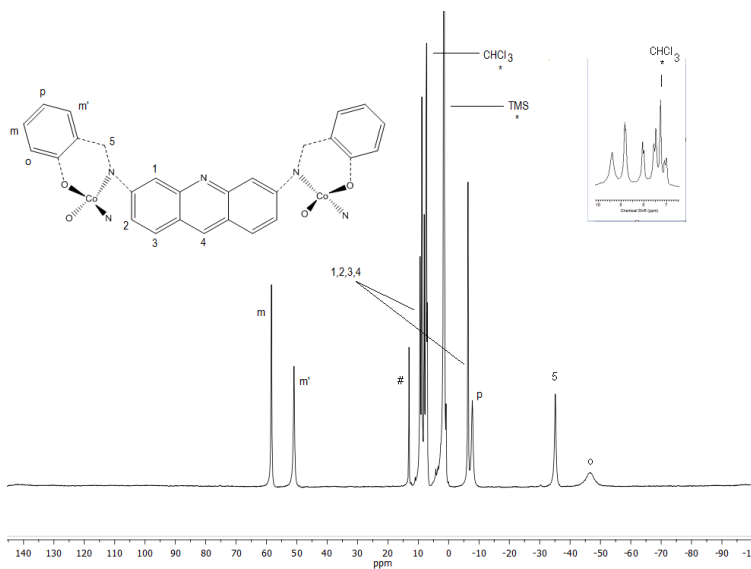


Figure 23. Complex 2  $^1\text{H}$  NMR paramagnetic spectrum. Protio impurity of the  $\text{CDCl}_3$  solvent is marked with asterisk. ACRI-2 hydrogen 11 is marked with a #.



## 8. CONCLUSIONS

The synthesis of multifunctional fluorescent and magnetic complexes (complex 1, 2, 3 and 4) has been successfully accomplished. In addition the reaction times and conditions have been optimized. This is particularly important for the synthesis of the ligands ACRI-1 and ACRI-2 which can now be obtained in high reproducible yield.

Complex 3 structure have been recorded also. Even though complex 1 and complex 3 are very similar, under the same crystallization conditions, their three dimensional arrangement is completely different.

It has been shown that complex 3 is a new fluorescent, magnetic and porous complex. A very interesting new world of possibilities has been opened and has to be studied. The channels are large, only in one direction, filled with solvents, and maybe with the possibility of removing these solvents.

Fluorescence emission spectra have been successfully recorded. Emission at 500-600 nm is obtained when the samples are irradiated with 350 nm light.

Electronic spectra consisted on two parts: the ligand aromatic absorbance (under 500 nm), and metal d-d forbidden bands (upper 500nm). Different concentrations have to be prepared to observe each one.



## 9. REFERENCES AND NOTES

1. Heras-Ojea, M. J.; Mañeru, D. R.; Rosado, L.; Zuazo, J. R.; Castro, G. R.; Tewary, S.; Rajaraman, G.; Aromí, G.; Jiménez, E.; Sañudo, E. C. "Characterization of a Robust Coll Fluorescent Complex Deposited Intact On HOPG" *Chemistry* 2014, 20, 10439–10445.
2. Menelaou, M.; Ouharrou, F.; Rodríguez, L.; Roubeau, O.; Teat, S. J.; Aliaga-Alcalde, N. "DyIII- and YbIII-Curcuminoid Compounds: Original Fluorescent Single-Ion Magnet and Magnetic Near-IR Luminescent Species" *Chemistry* 2012, 18, 11545–11549.
3. Heras-Ojea, M. J. Master Dissertation, Universitat de Barcelona, 2013
4. Mañeru, D. R.; Heras-Ojea, M. M.; Rosado, L.; Aromí, G.; Zuarzo, J.; Castro, G.; Sañudo, E. C. "New nanostructured materials: Nanostructuring of a fluorescent magnet based on acridine yellow" *Polyhedron* 2013, 66, 136-141.
5. Camarero, J.; Coronado, E. "Molecular vs. Inorganics pintronic: the role of molecular materials and single molecules" *Journal of Materials Chemistry* 2009, 19, 1678-1684.
6. Cosquer, G.; Pointillart, F.; Le Guennic, B.; Le Gal, Y.; Golhen, S.; Cador, O.; Ouahab, L. "3d4f Heterobimetallic Dinuclear and Tetranuclear Complexes Involving Tetrathiafulvalene as Ligands: X-ray structures and Magnetic and Photophysical Investigations" *American Chemical Society, Inorg. Chem.* 2012, 51, 8488-8501.
7. Professor Monzir Abdel-Latif webpage. Lab Manuals. Practical Instrumental Analysis. Molecular Fluorescence Spectroscopy. <http://www.monzir-pal.net/> (accessed Dec 22 2014).
8. Cotton, F. A.; Wilkinson, G.; Murillo, C. A.; Bochmann, M.; "ADVANCED INORGANIC CHEMISTRY", 6th ed.; Wiley-Interscience: United States of America, 1999.
9. Seko, T.; Ogura, K.; Kawakami, Y.; Sugino, H.; Toyotama, H.; Tanaka, J. "Excimer emission of anthracene, perylene, coronene and pyrene microcrystals dispersed in water" *Chemical Physics Letters* 1998, 291, 438-444.



## **10. ACRONYMS**

ESI-MS: Electrosprai ionisation mass spectroscopy.

UV-Vis: Ultraviolet visible.

IR: Infrared.

py: Pyridine.







